Journal of Computational and Applied Mathematics 404 (2022) 113273

Contents lists available at ScienceDirect

Journal of Computational and Applied Mathematics

journal homepage: www.elsevier.com/locate/cam

A parameter-uniform grid equidistribution method for singularly perturbed degenerate parabolic convection–diffusion problems

Sunil Kumar [a,*], Sumit [a], Jesus Vigo-Aguiar [b]

[a] Department of Mathematical Sciences, Indian Institute of Technology (BHU) Varanasi, Uttar Pradesh, India
[b] Department of Applied Mathematics, University of Salamanca, Salamanca, Spain

ARTICLE INFO

Article history:
Received 19 January 2020
Received in revised form 23 July 2020

Keywords:
Singular perturbation
Degenerate parabolic problems
Equidistribution principle
Upwind scheme
Parameter-uniform convergence

ABSTRACT

We consider a class of singularly perturbed degenerate parabolic convection–diffusion problems on a rectangular domain. A numerical method is constructed using the implicit Euler scheme on a uniform mesh in the time direction and the upwind finite difference scheme on a layer adaptive non-uniform mesh in the spatial direction. The layer adaptive non-uniform mesh in the spatial direction is generated through the equidistribution of a suitably chosen monitor function. We perform error analysis through the truncation error and barrier function approach and prove that the method is uniformly convergent with first order in both time and space. Numerical results are given in support of theoretical findings.

1. Introduction

We shall consider a class of singularly perturbed degenerate parabolic convection–diffusion problems with the perturbation parameter ε such that $0 < \varepsilon \ll 1$. Let the domain be $\bar{G} = G \cup \partial G$, where $G = \Omega \times (0, \mathcal{T}] = (0, 1) \times (0, \mathcal{T}]$ and $\partial G = \Gamma_b \cup \Gamma_r \cup \Gamma_l$ with $\Gamma_b = [0, 1]\times\{0\}$, $\Gamma_l = \{0\} \times (0, \mathcal{T}]$ and $\Gamma_r = \{1\} \times (0, \mathcal{T}]$. On this domain, we define the model problem as follows

$$\begin{cases} \mathcal{L}u(x,t) := (L_\varepsilon - \frac{\partial}{\partial t})u(x,t) = f(x,t), \quad (x,t) \in G, \\ u(x,0) = g_b(x), \ x \in \bar{\Omega}, \\ u(0,t) = g_l(t), \ u(1,t) = g_r(t), \ 0 < t \le \mathcal{T}, \end{cases} \tag{1.1}$$

where

$$\begin{cases} L_\varepsilon u(x,t) := \varepsilon \frac{\partial^2 u}{\partial x^2}(x,t) + a(x)\frac{\partial u}{\partial x}(x,t) - b(x,t)u(x,t), \\ a(x) = a_0(x)x^p, \ p \ge 1, \\ a_0(x)\big|_{\bar{\Omega}} \ge \underline{a} > 0, \\ b(x,t)\big|_{\bar{G}} \ge \beta > 0. \end{cases}$$

* Corresponding author.
E-mail addresses: skumar.iitd@gmail.com (S. Kumar), sumit.rs.mat16@iitbhu.ac.in (Sumit), jvigo@usal.es (J. Vigo-Aguiar).

https://doi.org/10.1016/j.cam.2020.113273
0377-0427/

The function f and the coefficients a_0 and b are assumed to be sufficiently smooth. Further, sufficient compatibility conditions at the corners are considered such that the parabolic problem (1.1) possesses a unique solution and it is sufficiently smooth [1]. The considered problem (1.1) is known as a boundary turning point problem, since at $x = 0$ the coefficient of the convective term satisfies $a(x) = 0$. The point $x = 0$ is called a simple turning point for $p = 1$, and a multiple turning point for $p > 1$. It is shown that $u = v + w$, where v and w satisfy [2,3]

$$\left\| \frac{\partial^{s+r} v}{\partial x^s \partial t^r} \right\|_{\bar{G}} \leq C(1 + \varepsilon^{1-\frac{s}{2}}),\ 0 \leq s + 2r \leq 3 \tag{1.2}$$

and

$$\left| \frac{\partial^{s+r} w}{\partial x^s \partial t^r} \right| \leq C\varepsilon^{-s/2} e^{-\sqrt{\beta}x/\sqrt{\varepsilon}},\ (x,t) \in \bar{G},\ 0 \leq s + 2r \leq 3. \tag{1.3}$$

Such problems arise in the modeling of heat flow and mass transport near an oceanic rise [4]. In [5], degenerate PDEs are developed on a non-rectangular domain for convection–diffusion problems without a turning point. Some multiple turning point problems are given in [6] that arise in the modeling of thermal boundary layers in a laminar flow.

It is quite well known that standard numerical methods on uniform meshes do not give an efficient solution for boundary layer problems. So, a new class of numerical methods, the so called parameter-uniform numerical methods have been developed in the literature [1,7–9]. For the numerical solution of the parabolic problem (1.1), in [10], a classical implicit upwind difference scheme on a piecewise-uniform Shishkin mesh in space and a uniform mesh in time is considered. In [2], the Richardson extrapolation technique is considered. In [3], a hybrid scheme on a piecewise-uniform Shishkin mesh in space and the backward Euler scheme on a uniform mesh in time is considered. In [11], a parameter-uniform numerical method is given for a discontinuous source term degenerate convection–diffusion singularly perturbed problem. In [12], the backward Euler method on a uniform mesh in time and a hybrid scheme on a generalized Shishkin mesh in space is considered.

Note that the numerical methods developed for the parabolic problem (1.1) in all the above papers use a priori refined meshes that are generated based on the location and width of the boundary layers. But, most of the time this a priori information about the solution is not available. Therefore, automatically generated layer adaptive meshes based on the equidistribution principle are quite effective for this case. Detailed literature on equidistribution meshes is available in [13–22].

To the best of our knowledge, we do not know of any paper that developed a parameter-uniform numerical method for the parabolic problem (1.1) based on automatically generated adaptive meshes. So, the main purpose of the paper is to construct a parameter-uniform numerical method for the parabolic problem (1.1) based on automatically generated adaptive meshes. Firstly, the problem is discretized in time using the implicit Euler scheme to get the linear stationary differential equations in the space variable. We prove first order parameter-uniform convergence in time for the semidiscrete scheme. After that, these differential equations are approximated using the standard upwind scheme on a non-uniform spatial mesh generated through the equidistribution principle. The monitor function that we consider in this paper is a combination of an appropriate power of second order derivative of the solution and a positive constant. We provide parameter-uniform convergence analysis of the method based on the truncation error and barrier function approach. It is shown that the method is first order parameter-uniformly convergent both in space and time. At the end, the method is implemented on two test examples to validate the theory.

The paper is organized as follows: In Section 2, we consider the semidiscretization of the parabolic problem (1.1) in time and prove that it is first order uniformly convergent. In Section 3, the layer adaptive spatial mesh is generated and the fully discrete scheme is given on this mesh. Section 4 is devoted to parameter-uniform convergence of the fully discrete scheme. In Section 5, we consider two test examples for validation of the theory.

Notation: We shall use C as a generic positive constant throughout the paper, which is independent of ε, space discretization parameter N and time discretization parameter M. We shall consider the maximum norm defined by $\max_{(x,t)\in D} |g(x,t)|$ for any function g defined on some domain D, and denote it by $\|g\|_D$. The discrete maximum norm is denoted by $\|g\|_{D^{N,M}}$.

2. The time semidiscretization

We consider the implicit Euler scheme to discretize the parabolic problem (1.1) on a uniform mesh with time step $\Delta t = \frac{T}{M}$, where M is taken to be the discretization parameter in the time direction. Thus, we define the temporal mesh $\bar{G}_t^M = \{t_m = m\Delta t, m = 0, \ldots, M\}$. The continuous problem (1.1) in semidiscretized form can be written as

$$\begin{cases} u^0(x) = g_b(x),\ x \in \bar{\Omega}, \\ \begin{cases} \text{For } m = 0, \ldots, M-1, \\ (\Delta t L_\varepsilon - I)u^{m+1}(x) = -u^m(x) + \Delta t f(x, t_{m+1}),\ x \in \Omega, \\ u^{m+1}(0) = g_l(t_{m+1}),\quad u^{m+1}(1) = g_r(t_{m+1}), \end{cases} \end{cases} \tag{2.1}$$

where I is the identity operator. We have the following minimum principle for the operator $(\Delta t L_\varepsilon - I)$.

Lemma 1 (*[3]*). *Consider the function $z^{m+1} \in C^2(\bar{\Omega})$ such that $z^{m+1}(0) \geq 0,\ z^{m+1}(1) \geq 0$, and $(\Delta t L_\varepsilon - I)z^{m+1}(x)|_\Omega \leq 0$. Then $z^{m+1}(x)|_{\bar{\Omega}} \geq 0$.*

The local truncation error of the time semidiscrete scheme (2.1) is given by $e_{m+1} = u(x, t_{m+1}) - \breve{u}^{m+1}(x)$, where $\breve{u}^{m+1}$ solves the following problem

$$\begin{cases} (\Delta t L_\varepsilon - I)\breve{u}^{m+1}(x) = -u(x, t_m) + \Delta t f(x, t_{m+1}),\ x \in \Omega, \\ \breve{u}^{m+1}(0) = g_l(t_{m+1}), \quad \breve{u}^{m+1}(1) = g_r(t_{m+1}). \end{cases} \tag{2.2}$$

Lemma 2. *The time derivatives of u satisfy the following bound*

$$\left\| \frac{\partial^s u}{\partial t^s} \right\|_{\bar{G}} \leq C, \quad 0 \leq s \leq 2.$$

Thus, the local error e_{m+1} satisfies

$$\|e_{m+1}\|_{\bar{\Omega}} \leq C(\Delta t)^2,$$

and the global error satisfies

$$\sup_{m+1 \leq \mathcal{T}/\Delta t} \|u(x, t_{m+1}) - u^{m+1}(x)\|_{\bar{\Omega}} \leq C\Delta t.$$

Proof. The time derivatives are bounded by using the arguments in [10]. The bounds on the local and global errors follow from the arguments in [23,24]. □

The above lemma entails the first order parameter-uniform convergence of the time semidiscretization process.

Lemma 3. *Consider the decomposition of $\breve{u}^{m+1}(x)$ as $\breve{u}^{m+1}(x) = \breve{v}^{m+1}(x) + \breve{w}^{m+1}(x)$, where $\breve{u}^{m+1},\ \breve{v}^{m+1}$, and $\breve{w}^{m+1}$ satisfy*

$$\left| \frac{\partial^s \breve{u}^{m+1}(x)}{\partial x^s} \right| \leq C(1 + \varepsilon^{-s/2} e^{-\sqrt{\beta}x/\sqrt{\varepsilon}}),$$

$$\left| \frac{\partial^s \breve{v}^{m+1}(x)}{\partial x^s} \right| \leq C(1 + \varepsilon^{1-\frac{s}{2}}),$$

$$\left| \frac{\partial^s \breve{w}^{m+1}(x)}{\partial x^s} \right| \leq C\varepsilon^{-s/2} e^{-\sqrt{\beta}x/\sqrt{\varepsilon}}, \quad 0 \leq s \leq 3,\ \textit{for all } x \in \bar{\Omega}.$$

Proof. The proof follows from the arguments in [3]. □

3. Spatial mesh generation and discretization

3.1. Layer adaptive equidistribution mesh

Here, we discuss the construction of a layer adaptive mesh through the equidistribution of a suitably chosen monitor function $\mathcal{M}(x, u(x, t_{m+1})) > 0$. A spatial mesh $\bar{G}_x^{N,m+1} = \{0 = x_0^{m+1}, x_1^{m+1}, \ldots, x_N^{m+1} = 1\}$ is said to be equidistributed if

$$\int_{x_{i-1}^{m+1}}^{x_i^{m+1}} \mathcal{M}(z, u(z, t_{m+1}))dz = \frac{1}{N} \int_0^1 \mathcal{M}(z, u(z, t_{m+1}))dz, \quad 1 \leq i \leq N.$$

In other form, mesh equidistribution can be seen as a mapping $x^{m+1} = x^{m+1}(\xi)$, which relates the computational coordinate $\xi \in [0, 1]$ to the physical coordinate $x^{m+1} \in [0, 1]$, defined by

$$\int_0^{x^{m+1}(\xi)} \mathcal{M}(z, u(z, t_{m+1}))dz = \xi \int_0^1 \mathcal{M}(z, u(z, t_{m+1}))dz. \tag{3.1}$$

Motivated from [17,19–22], we choose the monitor function given by

$$\mathcal{M}(x, u(x, t_{m+1})) = \alpha^{m+1} + \left| \frac{\partial^2 w}{\partial x^2}(x, t_{m+1}) \right|^{1/2}. \tag{3.2}$$

We note that α^{m+1} is a positive constant introduced to maintain the reasonable division of mesh points throughout the spatial domain. The equidistribution of the monitor function with $\alpha^{m+1} = 0$ results in mesh starvation outside the boundary layer regions. To approximate $\partial^2 w/\partial x^2$, we consider

$$\frac{\partial^2 w}{\partial x^2}(x, t_{m+1}) \approx \left(\frac{\eta}{\varepsilon}\right) e^{-\frac{\sqrt{\beta}x}{\sqrt{\varepsilon}}},$$

where η (independent of ε and x) is a constant. Hence

$$\int_0^1 \left|\frac{\partial^2 w}{\partial x^2}(x, t_{m+1})\right|^{1/2} dx \equiv \Lambda \approx 2|\eta|^{1/2}\beta^{-1/2}\left(1 - e^{-\frac{\sqrt{\beta}}{2\sqrt{\varepsilon}}}\right). \tag{3.3}$$

Now the equidistribution of (3.2) using definition (3.1) leads to the mapping

$$e^{\left(-\frac{\sqrt{\beta}}{2\sqrt{\varepsilon}}x^{m+1}(\xi)\right)} - \frac{\alpha^{m+1}}{\Lambda}x^{m+1}(\xi) = 1 - \left(\frac{\alpha^{m+1}}{\Lambda} + 1 - e^{(-\frac{\sqrt{\beta}}{2\sqrt{\varepsilon}})}\right)\xi. \tag{3.4}$$

A non-uniform mesh in physical coordinates $\{x_i^{m+1}\}_{i=0}^N$ corresponds to an equispaced mesh $\{\xi_i = i/N\}_{i=0}^N$ in computational coordinates. So, the above equation is written as

$$e^{\left(-\frac{\sqrt{\beta}}{2\sqrt{\varepsilon}}x_i^{m+1}\right)} - \frac{\alpha^{m+1}}{\Lambda}x_i^{m+1} = 1 - \left(\frac{\alpha^{m+1}}{\Lambda} + 1 - e^{(-\frac{\sqrt{\beta}}{2\sqrt{\varepsilon}})}\right)\frac{i}{N}. \tag{3.5}$$

Hence, the adaptively generated mesh-points are given by the solution of the non-linear algebraic equation (3.5). Throughout the rest of the paper, we take $\alpha^{m+1} = \Lambda$. Next, we provide some lemmas for important properties of the mesh structure.

Lemma 4. *Suppose that the mesh (3.5) is constructed by taking $\alpha^{m+1} = \Lambda$ and*

$$\frac{2\sqrt{\varepsilon}}{\sqrt{\beta}}N\ln N < 1. \tag{3.6}$$

Then

$$x_{N/2-1} < \frac{2\sqrt{\varepsilon}}{\sqrt{\beta}}\ln N < x_{N/2}.$$

Proof. Putting $\alpha^{m+1} = \Lambda$ and $x_i^{m+1} = \frac{2\sqrt{\varepsilon}}{\sqrt{\beta}}\ln N$ into (3.5) and simplifying for i, we get

$$i = \frac{N - \left(1 - \frac{2\sqrt{\varepsilon}}{\sqrt{\beta}}N\ln N\right)}{2 - e^{-\frac{\sqrt{\beta}}{2\sqrt{\varepsilon}}}}.$$

Now the proof immediately follows using the assumption (3.6). □

Lemma 5. *For $i = 1, \ldots, N/2 - 1$, we have*

$$h_i^{m+1} < \frac{6\sqrt{\varepsilon}}{\sqrt{\beta}(N - 2i)}.$$

Proof. The proof is based on the lower and upper bounds of x_i^{m+1} denoted by $\underline{x}_i^{m+1}$ and $\bar{x}_i^{m+1}$, respectively. From (3.5), we have

$$e^{\left(-\frac{\sqrt{\beta}}{2\sqrt{\varepsilon}}\bar{x}_i^{m+1}\right)} = 1 - \left(2 - e^{(-\frac{\sqrt{\beta}}{2\sqrt{\varepsilon}})}\right)\frac{i}{N}.$$

Hence

$$x_i^{m+1} < \bar{x}_i^{m+1} = -\frac{2\sqrt{\varepsilon}}{\sqrt{\beta}}\log\left(1 - S\frac{i}{N}\right), \tag{3.7}$$

where $S = \left(2 - e^{(-\frac{\sqrt{\beta}}{2\sqrt{\varepsilon}})}\right)$. Now we use the obtained upper bound in (3.5) to get

$$x_i^{m+1} > \underline{x}_i^{m+1} = -\frac{2\sqrt{\varepsilon}}{\sqrt{\beta}}\log\left(1 - S\frac{i}{N} - \frac{2\sqrt{\varepsilon}}{\sqrt{\beta}}\log\left(1 - S\frac{i}{N}\right)\right). \tag{3.8}$$

Thus, for $i = 1, \ldots, N/2 - 1$,

$$h_i^{m+1} < \bar{x}_i^{m+1} - \underline{x}_{i-1}^{m+1} = \frac{2\sqrt{\varepsilon}}{\sqrt{\beta}}\log\left(1 + \frac{S + \frac{2\sqrt{\varepsilon}}{\sqrt{\beta}}N\log\left(\frac{N}{N - S(i-1)}\right)}{N - Si}\right)$$
$$< \frac{2\sqrt{\varepsilon}}{\sqrt{\beta}}\log\left(1 + \frac{3}{N - 2i}\right) < \frac{6\sqrt{\varepsilon}}{\sqrt{\beta}(N - 2i)}. \quad \square$$

Lemma 6. *For the mesh generated using (3.5), mesh-widths h_i^{m+1}, $i = 1, \ldots, N$, satisfy*

$$h_i^{m+1} \le CN^{-1}.$$

Proof. From (3.2), we have that $\Lambda = \alpha^{m+1} \le \mathcal{M}(x, u(x, t_{m+1}))$. Now using the derivative bounds we get

$$\int_0^1 \mathcal{M}(x, u(x, t_{n+1}))dx \le C.$$

Thus, by the equidistribution principle, we get

$$\alpha^{m+1} h_i^{m+1} \le \int_{x_{i-1}^{m+1}}^{x_i^{m+1}} \mathcal{M}(x, u(x, t_{m+1}))dx = \frac{1}{N}\int_0^1 \mathcal{M}(x, u(x, t_{n+1}))dx \le CN^{-1}.$$

Hence, $h_i^{m+1} \le CN^{-1}$. □

3.2. The fully discrete scheme

Here, we shall discretize problem (2.1) on a non-uniform spatial mesh $\bar{G}_x^{N,m} = \{0 = x_0^m < x_1^m < \cdots < x_N^m = 1\}$, where m represents the time level and the step sizes are defined by $h_i^m = x_i^m - x_{i-1}^m$, $i = 1, \ldots, N$. On this spatial mesh, for any mesh function Y with $Y(x_i, t_m) = Y_i^m$, we consider the following difference operators

$$D_x^+ Y_i^m = \frac{Y_{i+1}^m - Y_i^m}{h_{i+1}^m}, \qquad D_x^- Y_i^m = \frac{Y_i^m - Y_{i-1}^m}{h_i^m}, \qquad \delta_x^2 Y_i^m = \frac{D_x^+ Y_i^m - D_x^- Y_i^m}{(h_i^m + h_{i+1}^m)/2}.$$

We shall use the term $U(x_i^{m+1}, t_m)$ in the discretization of (2.1) as it is found by the linear interpolation of $U(x_i^m, t_m)$, $i = 0, 1, \ldots, N$. Now the fully discrete scheme is given by

$$\begin{cases} U_i^0 = g_b(x_i^1), \text{ for } i = 0, \ldots, N, \\ \begin{cases} \text{For } m = 0, \ldots, M-1, \\ (\Delta t L_\varepsilon^N - I)U_i^{m+1} = -U(x_i^{m+1}, t_m) + \Delta t f(x_i^{m+1}, t_{m+1}), \text{ for } i = 1, \ldots, N-1, \\ U_0^{m+1} = g_l(t_{m+1}), \quad U_N^{m+1} = g_r(t_{m+1}), \end{cases} \end{cases} \tag{3.9}$$

where the discrete operator L_ε^N is defined by

$$L_\varepsilon^N U_i^{m+1} := \varepsilon \delta_x^2 U_i^{m+1} + a_i D_x^+ U_i^{m+1} - b_i^{m+1} U_i^{m+1}.$$

After rearrangement of the terms we can rewrite Eq. (3.9) as

$$\begin{aligned} &s_i^{m+1,-} U_{i-1}^{m+1} + s_i^{m+1,\star} U_i^{m+1} + s_i^{m+1,+} U_{i+1}^{m+1} = q_i^{m+1}, \ i = 1, \ldots, N-1, \\ &U_0^{m+1} = g_l(t_{m+1}), \quad U_N^{m+1} = g_r(t_{m+1}), \end{aligned} \tag{3.10}$$

where the coefficients $s_i^{m+1,-}$, $s_i^{m+1,\star}$ and $s_i^{m+1,+}$ are given by

$$\begin{aligned} s_i^{m+1,-} &= \frac{2\varepsilon\Delta t}{h_i^{m+1}(h_i^{m+1}+h_{i+1}^{m+1})}, \qquad s_i^{m+1,+} = \frac{2\varepsilon\Delta t}{h_{i+1}^{m+1}(h_i^{m+1}+h_{i+1}^{m+1})} + \frac{\Delta t a(x_i^{m+1})}{h_{i+1}}, \\ s_i^{m+1,\star} &= -1 - \Delta t b(x_i^{m+1}, t_{m+1}) - s_i^{m+1,-} - s_i^{m+1,+}, \quad q_i^{m+1} = -\widetilde{U}(x_i^{m+1}, t_m) + \Delta t f(x_i^{m+1}, t_{m+1}), \end{aligned}$$

and $\widetilde{U}$ denotes the piecewise-linear interpolant of U. Suppose $\widetilde{V}$ denotes the piecewise-linear interpolant of V. Then v is approximated as follows

$$\begin{aligned} &[\Delta t(a_i D_x^+ - b_i^{m+1}) - I]V_i^{m+1} = -\widetilde{V}(x_i^{m+1}, t_m) + \Delta t f(x_i^{m+1}, t_{m+1}), \text{ for } i = 1, \ldots, N-1, \\ &V_i^0 = g_b(x_i^1), i = 0, 1, \ldots, N, \quad V_N^{m+1} = g_r(t_{m+1}). \end{aligned} \tag{3.11}$$

4. Error analysis

We consider spatial discretization of problem (2.2) for error analysis. So, we consider the following difference equation

$$\begin{aligned} &(\Delta t L_\varepsilon^N - I)\breve{U}_i^{m+1} = s_i^{m+1,-}\breve{U}_{i-1}^{m+1} + s_i^{m+1,\star}\breve{U}_i^{m+1} + s_i^{m+1,+}\breve{U}_{i+1}^{m+1} = \breve{q}_i^{m+1}, \ i = 1, \ldots, N-1, \\ &\breve{U}_0^{m+1} = g_l(t_{m+1}), \quad \breve{U}_N^{m+1} = g_r(t_{m+1}), \end{aligned} \tag{4.1}$$

where $s_i^{m+1,-}$, $s_i^{m+1,\star}$, and $s_i^{m+1,+}$ are as defined in (3.10) and $\breve{q}_i^{m+1} = -u(x_i^{m+1}, t_m) + \Delta t f(x_i^{m+1}, t_{m+1})$. The operator $(\Delta t L_\varepsilon^N - I)$ satisfies the following discrete comparison principle which can be proved using the standard arguments.

Lemma 7 (*Discrete Comparison Principle*). *Suppose that the difference operator* $(\Delta t L_\varepsilon^N - I)$ *satisfies the following inequality*

$$(\Delta t L_\varepsilon^N - I)X_i^{m+1} \le (\Delta t L_\varepsilon^N - I)Y_i^{m+1}, \quad \text{for } i = 1, \dots, N-1,$$

with $X_0^{m+1} \ge Y_0^{m+1}$ *and* $X_N^{m+1} \ge Y_N^{m+1}$, *then* $X_i^{m+1} \ge Y_i^{m+1}$, *for* $i = 0, \dots, N$.

We decompose $\check{U}_i^{m+1}$ as follows

$$\check{U}_i^{m+1} = \check{V}_i^{m+1} + \check{W}_i^{m+1},$$

where

$$\begin{aligned} (\Delta t L_\varepsilon^N - I)\check{V}_i^{m+1} &= -v(x_i^{m+1}, t_m) + \Delta t f(x_i^{m+1}, t_{m+1}), \quad 1 \le i \le N-1,\ 1 \le m \le M-1, \\ \check{V}_0^{m+1} &= v(x_0^{m+1}, t_{m+1}),\ \check{V}_N^{m+1} = v(x_N^{m+1}, t_{m+1}), \end{aligned} \tag{4.2}$$

and

$$\begin{aligned} (\Delta t L_\varepsilon^N - I)\check{W}_i^{m+1} &= -w(x_i^{m+1}, t_m), \quad 1 \le i \le N-1,\ 1 \le m \le M-1, \\ \check{W}_0^{m+1} &= w(x_0^{m+1}, t_{m+1}),\ \check{W}_N^{m+1} = w(x_N^{m+1}, t_{m+1}). \end{aligned} \tag{4.3}$$

We will bound errors in the smooth and singular components separately and combine them with the help of a triangle inequality as follows

$$|\check{U}_i^{m+1} - \check{u}^{m+1}(x_i^{m+1})| \le |\check{V}_i^{m+1} - \check{v}^{m+1}(x_i^{m+1})| + |\check{W}_i^{m+1} - \check{w}^{m+1}(x_i^{m+1})|. \tag{4.4}$$

Next, we consider the discrete Padé approximation of the function $e^{-\frac{\sqrt{\beta}x_i^{m+1}}{2\sqrt{\varepsilon}}}$ and prove some technical results to be used later.

Lemma 8. *Consider a mesh function* T_i^{m+1} *such that*

$$T_0^{m+1} = 1, \quad T_i^{m+1} = \prod_{l=1}^{i}\left(1 + \frac{\sqrt{\beta}h_l^{m+1}}{2\sqrt{\varepsilon}}\right)^{-1}, \quad i = 1, \dots, N.$$

Then, for $i = 1, \dots, N-1$, *we have*

$$(\Delta t L_\varepsilon^N - I)T_i^{m+1} \le -\frac{C\Delta t}{2\sqrt{\varepsilon}/\sqrt{\beta} + h_{i+1}^{m+1}} T_i^{m+1}.$$

Proof. We have

$$\frac{T_i^{m+1} - T_{i-1}^{m+1}}{h_i^{m+1}} = -\frac{\sqrt{\beta}}{2\sqrt{\varepsilon}} T_i^{m+1}.$$

Applying the discrete operator $(\Delta t L_\varepsilon^N - I)$ to T_i^{m+1}, we get

$$\begin{aligned} (\Delta t L_\varepsilon^N - I)T_i^{m+1} &= \Delta t\left[\varepsilon\delta_x^2 T_i^{m+1} + a_i D_x^+ T_i^{m+1} - b_i^{m+1}T_i^{m+1}\right] - T_i^{m+1} \\ &= \Delta t\left\{\frac{2\varepsilon}{h_i^{m+1} + h_{i+1}^{m+1}}\left[-\frac{\sqrt{\beta}}{2\sqrt{\varepsilon}}T_{i+1}^{m+1} + \frac{\sqrt{\beta}}{2\sqrt{\varepsilon}}T_{i+1}^{m+1}\left(1 + \frac{\sqrt{\beta}h_{i+1}^{m+1}}{2\sqrt{\varepsilon}}\right)\right]\right. \\ &\quad \left. + a_i\left(\frac{-\sqrt{\beta}}{2\sqrt{\varepsilon}}\right)T_{i+1}^{m+1} - b_i^{m+1}T_i^{m+1}\right\} - T_i^{m+1} \\ &\le \frac{-\sqrt{\beta}\Delta t}{2\sqrt{\varepsilon} + \sqrt{\beta}h_{i+1}^{m+1}}\left[a_i - \frac{\sqrt{\varepsilon}\sqrt{\beta}h_{i+1}^{m+1}}{h_i^{m+1} + h_{i+1}^{m+1}} + \frac{b_i^{m+1}(2\sqrt{\varepsilon} + \sqrt{\beta}h_{i+1}^{m+1})}{\sqrt{\beta}}\right]T_i^{m+1} \\ &\le -\frac{\Delta t}{2\sqrt{\varepsilon}/\sqrt{\beta} + h_{i+1}^{m+1}}\left[a_i + \frac{\sqrt{\varepsilon}}{\sqrt{\beta}}(2b_i^{m+1} - \beta) + b_i^{m+1}h_{i+1}^{m+1}\right]T_i^{m+1} \\ &\le -\frac{C\Delta t}{2\sqrt{\varepsilon}/\sqrt{\beta} + h_{i+1}^{m+1}} T_i^{m+1}. \quad \square \end{aligned}$$

Lemma 9. *The mesh function* T_i^{m+1} *satisfies*

$$e^{-\frac{\sqrt{\beta}x_i^{m+1}}{2\sqrt{\varepsilon}}} \le T_i^{m+1}, \ i = 1, \dots, N. \tag{4.5}$$

Also,

$$T_{N/2-1}^{m+1} \le CN^{-1}.$$

Proof. We know that, for any positive real number y, $e^{-y} < 1/(1+y)$; so working for each i, we can easily get that

$$e^{-\frac{\sqrt{\beta}x_i^{m+1}}{2\sqrt{\varepsilon}}} = \prod_{l=1}^{i} e^{-\frac{\sqrt{\beta}h_l^{m+1}}{2\sqrt{\varepsilon}}} \le \prod_{l=1}^{i}\left(1+\frac{\sqrt{\beta}h_l^{m+1}}{2\sqrt{\varepsilon}}\right)^{-1} = T_i^{m+1}.$$

This proves (4.5). Now using the bound on the mesh sizes from Lemma 5, we have

$$\begin{aligned}\log\left(\prod_{l=1}^{N/2-1}\left(1+\frac{\sqrt{\beta}h_l^{m+1}}{2\sqrt{\varepsilon}}\right)\right) &= \sum_{l=1}^{N/2-1}\log\left(1+\frac{\sqrt{\beta}h_l^{m+1}}{2\sqrt{\varepsilon}}\right)\\ &> \sum_{l=1}^{N/2-1}\left(\frac{\sqrt{\beta}h_l^{m+1}}{2\sqrt{\varepsilon}} - \frac{1}{2}\left(\frac{\sqrt{\beta}h_l^{m+1}}{2\sqrt{\varepsilon}}\right)^2\right)\\ &> \frac{\sqrt{\beta}x_{N/2-1}^{m+1}}{2\sqrt{\varepsilon}} - \frac{9}{8}\sum_{l=1}^{N/2-1}\frac{1}{l^2} > \frac{\sqrt{\beta}x_{N/2-1}^{m+1}}{2\sqrt{\varepsilon}} - \frac{9}{4}.\end{aligned}$$

Thus

$$\prod_{l=1}^{N/2-1}\left(1+\frac{\sqrt{\beta}h_l^{m+1}}{2\sqrt{\varepsilon}}\right)^{-1} < e^{\frac{9}{4}-\frac{\sqrt{\beta}x_{N/2-1}^{m+1}}{2\sqrt{\varepsilon}}} < Ce^{-\frac{\sqrt{\beta}x_{N/2-1}^{m+1}}{2\sqrt{\varepsilon}}}.$$

Now from the mapping (3.5), we have

$$e^{-\frac{\sqrt{\beta}x_{N/2-1}^{m+1}}{2\sqrt{\varepsilon}}} = x_{N/2-1}^{m+1} + 1 - \frac{N-2}{2N}(2 - e^{-\frac{\sqrt{\beta}}{2\sqrt{\varepsilon}}}) < x_{N/2-1}^{m+1} + 2N^{-1} < \frac{2\sqrt{\varepsilon}}{\sqrt{\beta}}\log N + 2N^{-1}.$$

So, using assumption (3.6), we obtain

$$T_{N/2-1}^{m+1} \le CN^{-1}. \quad \square$$

4.1. Error analysis of the regular component

Lemma 10. *For $i = 0, \dots, N$, the error in the regular component $\check{V}_i^{m+1}$ satisfies*

$$|\check{V}_i^{m+1} - \check{v}^{m+1}(x_i^{m+1})| \le CN^{-1}.$$

Proof. The local truncation error at time level $m+1$ is given by

$$\begin{aligned}\eta_i^{m+1}(\check{V}) &= (\Delta t L_\varepsilon^N - I)(\check{V}_i^{m+1} - \check{v}^{m+1}(x_i^{m+1}))\\ &= \frac{\varepsilon\Delta t}{(h_i^{m+1}+h_{i+1}^{m+1})}\left[\frac{1}{h_{i+1}^{m+1}}\int_{x_i^{m+1}}^{x_{i+1}^{m+1}}(z-x_{i+1}^{m+1})^2\check{v}_{xxx}^{m+1}(z)dz - \frac{1}{h_i^{m+1}}\int_{x_{i-1}^{m+1}}^{x_i^{m+1}}(z-x_{i-1}^{m+1})^2\check{v}_{xxx}^{m+1}(z)dz\right]\\ &\quad + \frac{\Delta t\ a(x_i^{m+1})}{h_i^{m+1}}\int_{x_{i-1}^{m+1}}^{x_i^{m+1}}(z-x_{i+1}^{m+1})\check{v}_{xx}^{m+1}(z)dz.\end{aligned}$$

Thus

$$|\eta_i^{m+1}(\check{V})| \le \varepsilon\Delta t\int_{x_{i-1}^{m+1}}^{x_{i+1}^{m+1}}|\check{v}_{xxx}^{m+1}(z)|dz + a_{\max}\Delta t\int_{x_{i-1}^{m+1}}^{x_i^{m+1}}|\check{v}_{xx}^{m+1}(z)|dz,$$

where $a_{\max}$ is the maximum value of $a(x)$. Now using bounds on the derivatives (from Lemma 3) and the mesh sizes bound (from Lemma 6), we get

$$|\eta_i^{m+1}(\check{V})| \le CN^{-1}. \tag{4.6}$$

Now applying the operator $(\Delta t L_\varepsilon^N - I)$ to the barrier function $\Phi_i^\pm = CN^{-1} \pm (\check{V}_i^{m+1} - \check{v}^{m+1}(x_i^{m+1}))$, for $i = 1, \dots, N-1$, we get

$$(\Delta t L_\varepsilon^N - I)\Phi_i^\pm = -(\Delta t b_i^{m+1} + 1)CN^{-1} \pm (\Delta t L_\varepsilon^N - I)(\check{V}_i^{m+1} - \check{v}^{m+1}(x_i^{m+1})) \le 0,$$

with $\Phi_0^\pm \ge 0$ and $\Phi_N^\pm \ge 0$. Thus, using the discrete comparison principle, we get

$$|\check{V}_i^{m+1} - \check{v}^{m+1}(x_i^{m+1})| \le CN^{-1},\ i = 0, \dots, N. \quad \square$$

4.2. Error analysis of the singular component

4.2.1. Outside the layer region

Lemma 11. *For $i = N/2-1, \ldots, N$, it holds*

$$|\check{W}_i^{m+1} - \check{w}^{m+1}(x_i^{m+1})| \le CN^{-1}.$$

Proof. We use (4.3) and (1.3) to get

$$|\check{W}_N^{m+1}| \le Ce^{-\frac{\sqrt{\beta}}{\sqrt{\varepsilon}}} \le Ce^{-\frac{\sqrt{\beta}}{2\sqrt{\varepsilon}}} = C\prod_{l=1}^{N} e^{-\frac{\sqrt{\beta}h_l^{m+1}}{2\sqrt{\varepsilon}}}.$$

Then using the arguments of Lemma 9, we get $|\check{W}_N^{m+1}| \le CT_N^{m+1}$. Also, from (4.3), we get $|\check{W}_0^{m+1}| \le C \le CT_0^{m+1}$. Now

$$|(\Delta t L_\varepsilon^N - I)\check{W}_i^{m+1}| = |w(x_i^{m+1}, t_m)| \le Ce^{-\frac{\sqrt{\beta}x_i^{m+1}}{\sqrt{\varepsilon}}} \le Ce^{-\frac{\sqrt{\beta}x_i^{m+1}}{2\sqrt{\varepsilon}}} \le CT_i^{m+1},$$

where we have used (1.3) and Lemma 9. It is easy to verify that $(\Delta t L_\varepsilon^N - I)T_i^{m+1} \le -T_i^{m+1}$. Hence, an application of the discrete comparison principle with $\Psi_i^{\pm} = CT_i^{m+1} \pm \check{W}_i^{m+1}$ gives

$$|\check{W}_i^{m+1}| \le CT_i^{m+1}, \quad \text{for } i = 0, \ldots, N. \tag{4.7}$$

From Lemma 9, we have that $T_{N/2-1}^{m+1} \le CN^{-1}$. Since T_i^{m+1} decreases as i increases, so for $i = N/2-1, \ldots, N$, we have

$$T_i^{m+1} \le CN^{-1}. \tag{4.8}$$

Combining (4.7) and (4.8), we get

$$|\check{W}_i^{m+1}| \le CN^{-1}. \tag{4.9}$$

From Lemma 3, for $i = N/2-1, \ldots, N$,

$$|\check{w}^{m+1}(x_i^{m+1})| \le Ce^{-\frac{\sqrt{\beta}x_i^{m+1}}{\sqrt{\varepsilon}}} \le Ce^{-\frac{\sqrt{\beta}x_i^{m+1}}{2\sqrt{\varepsilon}}} \le Ce^{-\frac{\sqrt{\beta}x_{N/2-1}^{m+1}}{2\sqrt{\varepsilon}}} < CN^{-1}, \tag{4.10}$$

where we have used the fact from the proof of Lemma 9.

Thus, for the region outside the boundary layer, we obtain the desired result using Eqs. (4.9) and (4.10) in the following triangle inequality

$$|\check{W}_i^{m+1} - \check{w}^{m+1}(x_i^{m+1})| \le |\check{W}_i^{m+1}| + |\check{w}^{m+1}(x_i^{m+1})|. \quad \square$$

4.2.2. Inside the layer region

Lemma 12. *For $i = 1, \ldots, N/2-2$, we have*

$$|\check{W}_i^{m+1} - \check{w}^{m+1}(x_i^{m+1})| \le CN^{-1}.$$

Proof. Using Taylor expansions and the derivative bounds of $\check{w}^{m+1}$ from Lemma 3, we get

$$\begin{aligned}
|\eta_i^{m+1}(\check{W})| &\le \frac{C\Delta t}{\varepsilon}\int_{x_{i-1}^{m+1}}^{x_{i+1}^{m+1}} e^{-\frac{\sqrt{\beta}z}{\sqrt{\varepsilon}}}dz \le \frac{C\Delta t}{\varepsilon}\int_{\xi_{i-1}}^{\xi_{i+1}} \frac{Ae^{-\frac{\sqrt{\beta}x(\xi)}{\sqrt{\varepsilon}}}}{\alpha^{m+1} + |\check{w}_{xx}^{m+1}|^{1/2}}d\xi \\
&\le \frac{C\Delta t}{\sqrt{\varepsilon}}\int_{\xi_{i-1}}^{\xi_{i+1}} e^{-\frac{\sqrt{\beta}x(\xi)}{2\sqrt{\varepsilon}}}d\xi < \frac{C\Delta t}{\sqrt{\varepsilon}N}e^{-\frac{\sqrt{\beta}x_{i-1}^{m+1}}{2\sqrt{\varepsilon}}} = \frac{C\Delta t}{\sqrt{\varepsilon}N}e^{-\frac{\sqrt{\beta}x_i^{m+1}}{2\sqrt{\varepsilon}}}e^{\frac{\sqrt{\beta}h_i^{m+1}}{2\sqrt{\varepsilon}}}.
\end{aligned}$$

Also, from Lemma 5, we have $h_i^{m+1} < \frac{2\sqrt{\varepsilon}}{\sqrt{\beta}}\log\left(1 + \frac{3}{N-2i}\right)$. Thus, we get

$$|\eta_i^{m+1}(\check{W})| \le \frac{C\Delta t}{\sqrt{\varepsilon}N}e^{-\frac{\sqrt{\beta}x_i^{m+1}}{2\sqrt{\varepsilon}}}.$$

Again, using Lemma 9, we get

$$|\eta_i^{m+1}(\check{W})| \le \frac{C\Delta t}{\sqrt{\varepsilon}N}T_i^{m+1}.$$

Now we apply the discrete comparison principle to obtain an error bound for $\check{W}$. Consider $\psi_i^{m+1} = \frac{C}{N}(1 + T_i^{m+1}),\ i = 0, \ldots, N/2 - 1$. Then, using Lemmas 5 and 8, for $i = 1, \ldots, N/2 - 2$, we have

$$(\Delta t L_\varepsilon^N - I)(\check{W}_i^{m+1} - \check{w}^{m+1}(x_i^{m+1})) = \eta_i^{m+1}(\check{W}) \geq -\frac{C\Delta t}{\sqrt{\varepsilon}N} T_i^{m+1} \geq \frac{C}{N}(\Delta t L_\varepsilon^N - I)T_i^{m+1} \geq (\Delta t L_\varepsilon^N - I)\psi_i^{m+1}.$$

Also,

$$(\check{W}_0^{m+1} - \check{w}^{m+1}(x_0^{m+1})) \leq \psi_0^{m+1} \quad \text{and} \quad (\check{W}_{N/2-1}^{m+1} - \check{w}^{m+1}(x_{N/2-1}^{m+1})) \leq \psi_{N/2-1}^{m+1}.$$

Hence, using the discrete comparison principle, we have

$$(\check{W}_i^{m+1} - \check{w}^{m+1}(x_i^{m+1})) \leq \psi_i^{m+1},\ i = 0, \ldots, N/2 - 1,$$

which implies that

$$(\check{W}_i^{m+1} - \check{w}^{m+1}(x_i^{m+1})) \leq CN^{-1},\ i = 1, \ldots, N/2 - 2.$$

Now we repeat the above argument for $-(\check{W}_i^{m+1} - \check{w}^{m+1}(x_i^{m+1}))$. Thus, we have

$$|\check{W}_i^{m+1} - \check{w}^{m+1}(x_i^{m+1})| \leq CN^{-1},\ i = 1, \ldots, N/2 - 2. \quad \square$$

Theorem 4.1. *Suppose $\check{u}^{m+1}(x_i^{m+1})$ and $\check{U}_i^{m+1}$, respectively, are the solutions of (2.1) and (4.1). Then on the equidistribution mesh (3.5), we have*

$$|\check{U}_i^{m+1} - \check{u}^{m+1}(x_i^{m+1})| \leq CN^{-1},\quad i = 0, \ldots, N.$$

Proof. The result follows by using Lemmas 10, 11, and 12 in the inequality (4.4). $\square$

Corollary 4.1. *If for some $0 < \sigma < 1,\ N^{-\sigma} \leq C\Delta t$, then from the previous theorem we have*

$$|\check{U}_i^{m+1} - \check{u}^{m+1}(x_i^{m+1})| \leq C\Delta t N^{-1+\sigma},\quad i = 0, \ldots, N.$$

The constant σ in the above corollary does not influence numerical results given in the next section, and is used only for the theory. Such an assumption is common in the literature (see, e.g. [23,25]). In the following theorem, we prove parameter-uniform convergence of the fully discrete scheme. The analysis in this theorem is inspired from the works in [23,25].

Theorem 4.2. *Suppose u is the solution of (1.1) and $\{U_i^{m+1}\}$ is the solution of the fully discrete scheme (3.9) at the $(m+1)$th time level. If for some $0 < \sigma < 1,\ N^{-\sigma} \leq C\Delta t$, then on each time level t_{m+1} we have*

$$\|U_i^{m+1} - u(x_i^{m+1}, t_{m+1})\|_{\bar{G}_x^{N,m+1}} \leq C(N^{-1+\sigma} + M^{-1}).$$

Proof. We define the error of the fully discrete scheme at time level t_{m+1} by $E_i^{m+1} = U_i^{m+1} - u(x_i^{m+1}, t_{m+1}), 0 \leq i \leq N$. We can split the global error as follows

$$\begin{aligned}\|E_i^{m+1}\|_{\bar{G}_x^{N,m+1}} \leq{}& \|U_i^{m+1} - \check{U}_i^{m+1}\|_{\bar{G}_x^{N,m+1}} + \|\check{U}_i^{m+1} - \check{u}^{m+1}(x_i^{m+1})\|_{\bar{G}_x^{N,m+1}} \\ &+ \|\check{u}^{m+1}(x_i^{m+1}) - u(x_i^{m+1}, t_{m+1})\|_{\bar{G}_x^{N,m+1}}.\end{aligned}$$

Using the results from Lemma 2 and Corollary 4.1, we obtain

$$\|E^{m+1}\|_{\bar{G}_x^{N,m+1}} \leq \|U_i^{m+1} - \check{U}_i^{m+1}\|_{\bar{G}_x^{N,m+1}} + C\Delta t(\Delta t + N^{-1+\sigma}). \tag{4.11}$$

Now considering (3.9), (4.1), and the stability of $(\Delta t L_\varepsilon^N - I)$, we get

$$\|U_i^{m+1} - \check{U}_i^{m+1}\|_{\bar{G}_x^{N,m+1}} \leq \|\widetilde{U}(x_i^{m+1}, t_m) - u(x_i^{m+1}, t_m)\|_{\bar{G}_x^{N,m+1}}.$$

Then using a triangle inequality we get

$$\|\widetilde{U}(x_i^{m+1}, t_m) - u(x_i^{m+1}, t_m)\|_{\bar{G}_x^{N,m+1}} \leq \|\widetilde{U}(x_i^{m+1}, t_m) - \tilde{u}(x_i^{m+1}, t_m)\|_{\bar{G}_x^{N,m+1}} + \|\tilde{u}(x_i^{m+1}, t_m) - u(x_i^{m+1}, t_m)\|_{\bar{G}_x^{N,m+1}}. \tag{4.12}$$

The second term on right hand side of (4.12) is the interpolation error. Using standard arguments we get $\|\tilde{u}(x_i^{m+1}, t_m) - u(x_i^{m+1}, t_m)\|_{\bar{G}_x^{N,m+1}} \leq CN^{-1}$, and hence

$$\|\tilde{u}(x_i^{m+1}, t_m) - u(x_i^{m+1}, t_m)\|_{\bar{G}_x^{N,m+1}} \leq C\Delta t N^{-1+\sigma},\ \text{for some } 0 < \sigma < 1 \text{ such that } N^{-\sigma} \leq C\Delta t.$$

The first term on right hand side of (4.12) is bounded using the stability of the interpolation operator. So, we get

$$\|\widetilde{U}(x_i^{m+1}, t_m) - \tilde{u}(x_i^{m+1}, t_m)\|_{\bar{G}_x^{N,m+1}} \leq \|U_i^m - u(x_i^m, t_m)\|_{\bar{G}_x^{N,m}}.$$

Thus

$$\|E^{m+1}\|_{\bar{G}_x^{N,m+1}} \leq \|E^m\|_{\bar{G}_x^{N,m}} + C\Delta t(\Delta t + N^{-1+\sigma}).$$

Hence, using a recursive argument, we obtain

$$\|E^{m+1}\|_{\bar{G}_x^{N,m+1}} \leq C(\Delta t + N^{-1+\sigma}). \quad \square$$

5. Numerical results

We present numerical results for two test examples to validate the theory. To generate adaptive meshes we consider a moving mesh algorithm originally due to de Boor [26]. Starting with a uniform mesh the algorithm aims to construct a mesh that solves the following discrete equidistribution principle

$$h_i^m \mathcal{M}_i^m = \frac{1}{N}\sum_{j=1}^{N} h_j^m \mathcal{M}_j^m, \quad 1 \leq i \leq N, \tag{5.1}$$

where $\mathcal{M}_i^m$ is the discretized monitor function corresponding to (3.2). Kopteva and Stynes [27] remarked that the discrete equidistribution principle does not have to been enforced strictly, but it suffices to have

$$h_i^m \mathcal{M}_i^m \leq \frac{\varrho}{N}\sum_{j=1}^{N} h_j^m \mathcal{M}_j^m, \quad 1 \leq i \leq N, \tag{5.2}$$

with a user-chosen constant $\varrho > 1$.

We note that the moving mesh algorithm considered in this paper has been utilized for several classes of singularly perturbed problems in the literature (see [18,20–22,27,28] and the references therein). However, there are only a few attempts to analyze its convergence. The algorithm is analyzed in [29] for a stationary semilinear reaction–diffusion problem, in [27] for a stationary quasilinear convection–diffusion problem, and in [30] for regular boundary value problems. The following algorithm is used to generate the adaptive mesh and the solution at each time level.

Algorithm.

Step 1. Choose a stopping constant $\varrho > 1$. Initialize the mesh iteration $\{x_i^{m,(k)}\}$ with $k = 0$ as the uniform mesh for $m = 1$, otherwise x_i^{m-1} for the mth time level.

Step 2. Solve the discrete problem (3.9) for $U_i^{m,(k)}$ and (3.11) for smooth component $V_i^{m,(k)}$ on the spatial mesh $\{x_i^{m,(k)}\}$.

Step 3. Compute the singular component as $W_i^{m,(k)} = U_i^{m,(k)} - V_i^{m,(k)}$.

Step 4. Construct the discretized monitor function by

$$\mathcal{M}_i^{m,(k)} = \alpha^{m,(k)} + |\delta_x^2 W_i^{m,(k)}|^{1/2}, \quad \text{for } i = 1, \ldots, N-1,$$

where $\alpha^{m,(k)}$ is defined by

$$\alpha^{m,(k)} = h_1^{m,(k)}|\delta_x^2 W_1^{m,(k)}|^{1/2} + \sum_{i=2}^{N-1} h_i^{m,(k)} \left\{ \frac{|\delta_x^2 W_{i-1}^{m,(k)}|^{1/2} + |\delta_x^2 W_i^{m,(k)}|^{1/2}}{2} \right\} + h_N^{m,(k)}|\delta_x^2 W_{N-1}^{m,(k)}|^{1/2}.$$

Step 5. Set $H_i^{m,(k)} = h_i^{m,(k)}\left(\frac{\mathcal{M}_{i-1}^{m,(k)} + \mathcal{M}_i^{m,(k)}}{2}\right)$, for $i = 1, \ldots, N$; take $\mathcal{M}_0^{m,(k)} = \mathcal{M}_1^{m,(k)}$ and $\mathcal{M}_N^{m,(k)} = \mathcal{M}_{N-1}^{m,(k)}$. Now define $L_i^{m,(k)}$ by $L_i^{m,(k)} = \sum_{j=1}^{i} H_j^{m,(k)}$, for $i = 1, \ldots, N$, and $L_0^{m,(k)} = 0$.

Step 6. **Stopping criteria**: Define $\varrho^{(k)}$ by $\varrho^{(k)} = \frac{N}{L_N^{m,(k)}} \max_{i=1,\ldots,N} H_i^{m,(k)}$. If $\varrho^{(k)} \leq \varrho$ then go to Step 8, else continue with Step 7.

Step 7. Set $Z_i^{m,(k)} = i\frac{L_N^{m,(k)}}{N}$ for $i = 0, 1, \ldots, N$. Interpolate the points $(L_i^{m,(k)}, x_i^{m,(k)})$. Generate a new mesh $\{x_i^{m,(k+1)}\}$ by evaluating this interpolant at $Z_i^{m,(k)}$ for $i = 0, 1, \ldots, N$, then return to Step 2, setting $k = k + 1$.

Step 8. Take $\{x_i^{m,(k)}\}$ as the final layer adaptive mesh $\{x_i^m\}$ for the mth level and $U_i^{m,(k)}$ as the required adaptive solution U_i^m at the mth time level.

Step 9. Go to Step 1 with $m = m + 1$, repeat the same process for the adaptive mesh and solution at the $(m+1)$th time level.

Throughout this section we take $\mathcal{T} = 1$, $M = N$, and the stopping constant $\varrho = 1.05$, for all the numerical experiments. The first test example is the following degenerate convection–diffusion singular perturbation problem [2].

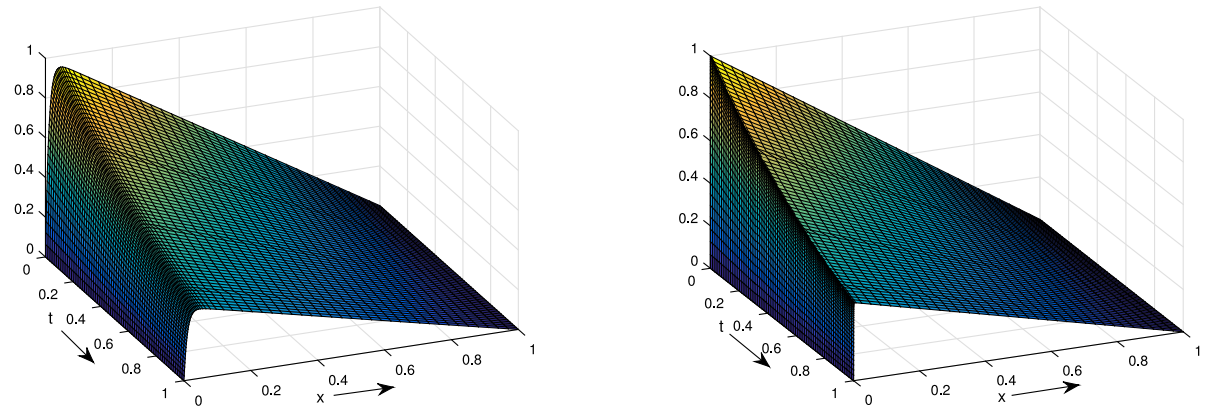

Fig. 1. Surface plots of the numerical solution of Example 5.1 with $N = 64$ and $p = 2$. The left figure is corresponding to $\varepsilon = 10^{-4}$ and the right figure is corresponding to $\varepsilon = 10^{-8}$.

Example 5.1.

$$\begin{cases} \varepsilon \frac{\partial^2 u}{\partial x^2}(x,t) + x^p \frac{\partial u}{\partial x}(x,t) - u(x,t) - \frac{\partial u}{\partial t}(x,t) = f(x,t), \quad (x,t) \in G, \\ u(x,t) = g(x,t), \quad (x,t) \in \partial G. \end{cases}$$

The functions f and g can be calculated from the exact solution

$$u(x,t) = e^{-t}\left(1 - x + xe^{-1/\sqrt{\varepsilon}} - e^{-x/\sqrt{\varepsilon}}\right).$$

Fig. 1 displays the surface plots for $\varepsilon = 10^{-4}$ and $\varepsilon = 10^{-8}$ with $N = 64$ and $p = 2$. From this figure one can clearly observe a boundary layer near Γ_l. For different values of M, N, and ε, we calculate the pointwise errors using the formula

$$E_{i,m}^{\varepsilon,N,M} = |U_i^{m;N,M} - u(x_i^m, t_m)|.$$

We then calculate the maximum pointwise errors and the numerical rates of convergence by

$$E^{\varepsilon,N,M} = \max_{i,m} E_{i,m}^{\varepsilon,N,M}, \qquad \rho^{\varepsilon,N,M} = \log_2\left(\frac{E^{\varepsilon,N,M}}{E^{\varepsilon,2N,2M}}\right).$$

Finally, the parameter-uniform errors and the parameter-uniform rates of convergence are computed by

$$E^{N,M} = \max_{\varepsilon} E^{\varepsilon,N,M}, \qquad \rho^{N,M} = \log_2\left(\frac{E^{N,M}}{E^{2N,2M}}\right).$$

In Table 1, we display the errors $E^{\varepsilon,N,M}$ and $E^{N,M}$, and the convergence rates $\rho^{\varepsilon,N,M}$ and $\rho^{N,M}$. Here, we see that the error is decreasing as the number of mesh points are increasing. From this table one can conclude that the method is parameter-uniform and the numerical results are in accordance with the theoretical result.

In Fig. 2, we plot the movement of mesh points towards the boundary layer in each iteration of the mesh generation process and the final position of mesh points condensed in the layer region. This figure confirms the adaptive behavior of the mesh obtained through the equidistribution of our chosen monitor function.

The second test example is the following degenerate convection–diffusion singular perturbation problem [5].

Example 5.2.

$$\begin{cases} \varepsilon \frac{\partial^2 u}{\partial x^2}(x,t) + x^p \frac{\partial u}{\partial x}(x,t) - u(x,t) - \frac{\partial u}{\partial t}(x,t) = x^2 - 1, \quad (x,t) \in G, \\ u(x,0) = (1-x)^2, \quad x \in \bar{\Omega}, \\ u(0,t) = 1 + t^2, \ u(1,t) = 0, \ 0 < t \le \mathcal{T}. \end{cases}$$

Fig. 3 displays the surface plot for $\varepsilon = 10^{-2}$ and $\varepsilon = 10^{-5}$ with $N = 64$ and $p = 2$, from which a boundary layer can be clearly observed near Γ_l. The exact solution of Example 5.2 is not known, so to estimate numerical errors and rates of convergence we shall use the double mesh principle [8]. For this we bisect the spatial mesh and the time mesh, and then calculate the pointwise errors using the formula

$$E_{i,m}^{\varepsilon,N,M} = |U_{2i}^{2m;2N,2M} - U_i^{m;N,M}|.$$

Table 1
Maximum pointwise errors $E^{\varepsilon,N,M}$, parameter-uniform errors $E^{N,M}$, rates of convergence $\rho_{\varepsilon}^{N,M}$, and parameter-uniform convergence rates $\rho^{N,M}$ using scheme (3.9) for Example 5.1 with $p = 2$.

ε	$N = 32$	$N = 64$	$N = 128$	$N = 256$	$N = 512$	$N = 1024$
10^{-1}	1.1134e−03	5.9091e−04	3.0455e−04	1.5456e−04	7.7859e−05	3.9075e−05
	0.9139	0.9563	0.9785	0.9892	0.9946	
10^{-2}	1.6582e−03	7.9905e−04	3.9089e−04	1.9332e−04	9.6135e−05	4.7937e−05
	1.0532	1.0315	1.0158	1.0078	1.0039	
10^{-3}	3.8784e−03	1.9835e−03	1.0078e−03	5.0731e−04	2.5449e−04	1.2724e−04
	0.9674	0.9769	0.9902	0.9952	1.0000	
10^{-4}	4.8593e−03	2.4942e−03	1.2707e−03	6.4185e−04	3.2171e−04	1.6086e−04
	0.9622	0.9729	0.9854	0.9965	1.0000	
10^{-5}	5.2579e−03	2.6824e−03	1.3657e−03	6.8888e−04	3.4636e−04	1.7313e−04
	0.9709	0.9739	0.9873	0.9920	1.0004	
10^{-6}	5.4821e−03	2.7604e−03	1.4010e−03	7.0610e−04	3.5561e−04	1.7758e−04
	0.9899	0.9784	0.9885	0.9896	1.0018	
10^{-7}	5.5818e−03	2.7898e−03	1.4162e−03	7.1248e−04	3.5910e−04	1.7919e−04
	1.0005	0.9781	0.9912	0.9885	1.0029	
10^{-8}	5.5841e−03	2.7974e−03	1.4199e−03	7.1555e−04	3.6052e−04	1.7976e−04
	0.9946	0.9783	0.9887	0.9890	1.0040	
$E^{N,M}$	5.5841e−03	2.7974e−03	1.4199e−03	7.1555e−04	3.6052e−04	1.7976e−04
$\rho^{N,M}$	0.9946	0.9783	0.9887	0.9890	1.0040	

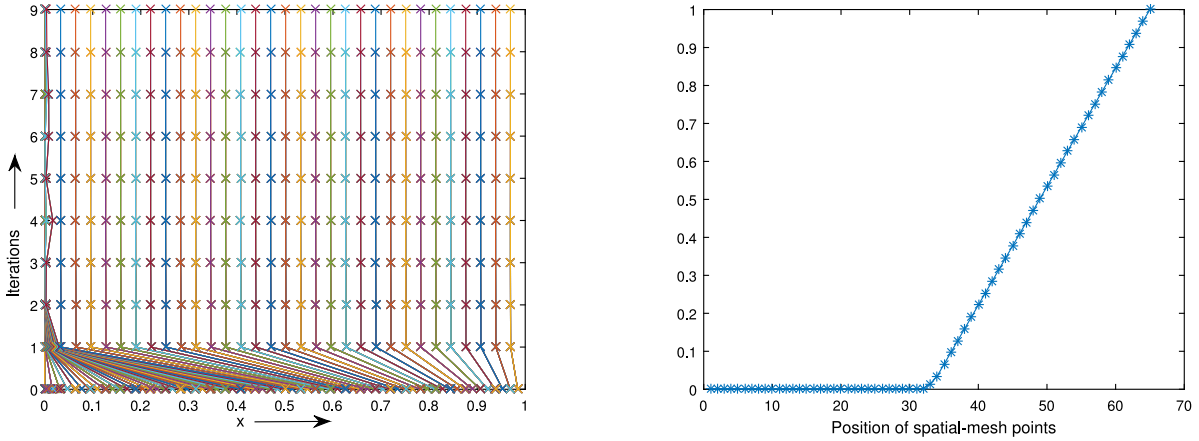

Fig. 2. Mesh trajectory and position of mesh points in space at $t = 1$ taking $\varepsilon = 10^{-8}$, $N = 64$, and $p = 2$ for Example 5.1.

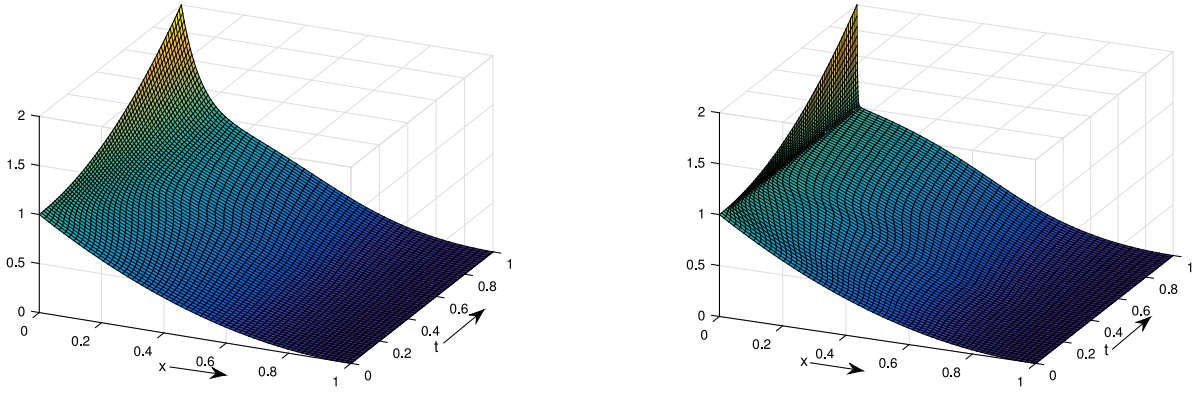

Fig. 3. Surface plots of the numerical solution of Example 5.2 with $N = 64$ and $p = 2$. The left figure is corresponding to $\varepsilon = 10^{-2}$ and the right figure is corresponding to $\varepsilon = 10^{-5}$.

Then the maximum pointwise errors and the rates of convergence are calculated by

$$E^{\varepsilon,N,M} = \max_{i,m} E_{i,m}^{\varepsilon,N,M}, \qquad \rho^{\varepsilon,N,M} = \log_2\left(\frac{E^{\varepsilon,N,M}}{E^{\varepsilon,2N,2M}}\right).$$

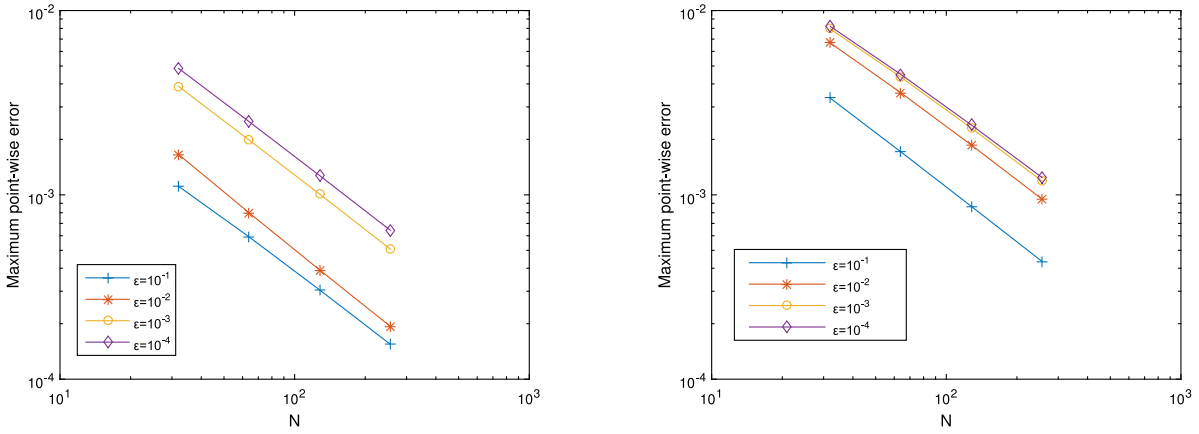

Fig. 4. Log–log plots of the maximum pointwise errors at time $t = 1$ for Examples 5.1 (in the left) and 5.2 (in the right), respectively.

Table 2
Maximum pointwise errors $E^{\varepsilon,N,M}$, parameter-uniform errors $E^{N,M}$, rates of convergence $\rho_{\varepsilon}^{N,M}$, and parameter-uniform convergence rates $\rho^{N,M}$ using scheme (3.9) for Example 5.2 with $p = 1$.

ε	$N = 32$	$N = 64$	$N = 128$	$N = 256$	$N = 512$	$N = 1024$
10^{-1}	6.0678e−03	3.1060e−03	1.5716e−03	7.9055e−04	3.9646e−04	1.9852e−04
	0.9661	0.9828	0.9913	0.9957	0.9979	
10^{-2}	9.1940e−03	4.8423e−03	2.4863e−03	1.2594e−03	6.3381e−04	3.1793e−04
	0.92501	0.9617	0.9812	0.9906	0.9953	
10^{-3}	1.1452e−02	6.2810e−03	3.2832e−03	1.6747e−03	8.4525e−04	4.2453e−04
	0.9669	0.9356	0.9711	0.98650	0.9935	
10^{-4}	1.4429e−02	7.8765e−03	4.1433e−03	2.1086e−03	1.0578e−03	5.2844e−04
	0.8734	0.9268	0.9745	0.9951	1.0013	
10^{-5}	1.8039e−02	9.3421e−03	4.9472e−03	2.5223e−03	1.2580e−03	6.2199e−04
	0.9493	0.9172	0.9718	1.0035	1.0161	
10^{-6}	2.2009e−02	1.0476e−02	5.5412e−03	2.8546e−03	1.4341e−03	7.0988e−04
	1.0710	0.9188	0.9569	0.9931	1.0145	
10^{-7}	2.5967e−02	1.1221e−02	5.8996e−03	3.0621e−03	1.5543e−03	7.7683e−04
	1.2104	0.9275	0.9461	0.9783	1.0001	
10^{-8}	2.9611e−02	1.1848e−02	6.1079e−03	3.1723e−03	1.6194e−03	8.1577e−04
	1.3215	0.9359	0.9451	0.9701	0.9892	
10^{-9}	3.0056e−02	1.1903e−02	6.1538e−03	3.2087e−03	1.6475e−03	8.1877e−04
	1.3363	0.9518	0.9395	0.9617	1.0087	
10^{-10}	3.0424e−02	1.1930e−02	6.1602e−03	3.2108e−03	1.6504e−03	8.1901e−04
	1.3506	0.9535	0.9400	0.9601	1.0109	
10^{-11}	3.0430e−02	1.1938e−02	6.1610e−03	3.2113e−03	1.6509e−03	8.1908e−04
	1.3499	0.9543	0.9400	0.9599	1.0112	
$E^{N,M}$	3.0430e−02	1.1938e−02	6.1610e−03	3.2113e−03	1.6509e−03	8.1908e−04
$\rho^{N,M}$	1.3499	0.9543	0.9400	0.9599	1.0112	

Finally, the parameter-uniform errors and the parameter-uniform rates of convergence are obtained by

$$E^{N,M} = \max_{\varepsilon} E^{\varepsilon,N,M}, \qquad \rho^{N,M} = \log_2\left(\frac{E^{N,M}}{E^{2N,2M}}\right).$$

In Table 2, we present the results for Example 5.2. This table displays the errors $E^{\varepsilon,N,M}$ and $E^{N,M}$, and the convergence rates $\rho^{\varepsilon,N,M}$ and $\rho^{N,M}$. From these numerical results, again we observe that the method is first order parameter-uniform for the addressed problem (1.1).

In Fig. 4, we provide log–log plots between the maximum pointwise errors and the number of spatial mesh points N, for both the test examples. From the slopes of these plots we can also validate first order convergence of the method.

In Table 3, we present the results for different values of ϱ for Example 5.1 taking $\varepsilon = 10^{-7}$. This table displays the maximum pointwise errors $E^{\varepsilon,N,M}$, convergence rates $\rho^{\varepsilon,N,M}$, and the maximum number of iterations required (over all time levels) before the stopping criterion in Step 6 of the algorithm is satisfied. From this table, we observe that values of ϱ close to 1 give slightly more accurate solutions but require more number of iterations. Further, we observe that the algorithm requires few iterations to converge.

Table 3
Maximum pointwise errors $E^{\varepsilon,N,M}$, rates of convergence $\rho_{\varepsilon}^{N,M}$, and the maximum number of iterations (over all time levels) K using different values of ϱ for Example 5.1 with $p = 2$ and $\varepsilon = 10^{-7}$.

ϱ		$N = 32$	$N = 64$	$N = 128$	$N = 256$	$N = 512$	$N = 1024$
$\varrho = 1.05$	$E^{\varepsilon,N,M}$	5.5818e−03	2.7898e−03	1.4162e−03	7.1248e−04	3.5910e−04	1.7918e−04
	$\rho^{\varepsilon,N,M}$	1.0005	0.9781	0.9912	0.9885	1.0029	
	K	12	7	7	6	5	4
$\varrho = 1.15$	$E^{\varepsilon,N,M}$	6.1339e−03	2.9877e−03	1.4609e−03	7.2179e−04	3.5916e−04	1.7919e−04
	$\rho^{\varepsilon,N,M}$	1.0378	1.0322	1.0172	1.0070	1.0031	
	K	10	6	5	5	4	3
$\varrho = 1.5$	$E^{\varepsilon,N,M}$	6.2798e−03	3.0429e−03	1.4616e−03	7.2169e−04	3.5900e−04	1.7919e−04
	$\rho^{\varepsilon,N,M}$	1.0453	1.0579	1.0181	1.0074	1.0025	
	K	6	5	4	4	3	3
$\varrho = 2.0$	$E^{\varepsilon,N,M}$	6.3449e−03	3.0370e−03	1.4616e−03	7.2079e−04	3.5900e−04	1.7919e−04
	$\rho^{\varepsilon,N,M}$	1.0629	1.0551	1.0199	1.0056	1.0025	
	K	4	4	4	3	3	3
$\varrho = 3.0$	$E^{\varepsilon,N,M}$	6.3449e−03	3.0370e−03	1.4616e−03	7.2079e−04	3.5900e−04	1.7919e−04
	$\rho^{\varepsilon,N,M}$	1.0629	1.0551	1.0199	1.0056	1.0025	
	K	4	4	4	3	3	3

6. Conclusion

We have proposed a numerical method comprising of the implicit Euler scheme on a uniform mesh in the time direction and the upwind finite difference scheme on a layer adaptive nonuniform mesh in the spatial direction, for solving degenerate singularly perturbed convection–diffusion problem. The layer adaptive non-uniform mesh in the spatial direction is generated through the equidistribution of the monitor function which is a combination of an appropriate power of second order derivative of the solution and a positive constant. It is shown through the truncation error and barrier function approach that the proposed method is parameter-uniform with first order in both time and space. Numerical results are given for two test examples which validate the theoretical findings.

Acknowledgments

This research was supported by the Science and Engineering Research Board (SERB), India under the Project No. ECR/2017/000564. The second author gratefully acknowledges the support of University Grant Commission, India, for research fellowship with reference No.: 20/12/2015(ii)EU-V. The authors gratefully acknowledge the valuable comments and suggestions from the anonymous referees.

References

[1] H.-G. Roos, M. Stynes, L. Tobiska, Robust Numerical Methods for Singularly Perturbed Differential Equations: Convection–Diffusion-Reaction and Flow Problems, Vol. 24, Springer Science & Business Media, 2008.
[2] A. Majumdar, S. Natesan, Second-order uniformly convergent richardson extrapolation method for singularly perturbed degenerate parabolic PDEs, Int. J. Appl. Comput. Math. 3 (1) (2017) 31–53.
[3] A. Majumdar, S. Natesan, An ε-uniform hybrid numerical scheme for a singularly perturbed degenerate parabolic convection–diffusion problem, Int. J. Comput. Math. 96 (7) (2019) 1313–1334.
[4] T.C. Hanks, Model relating heat-flow values near, and vertical velocities of mass transport beneath, oceanic rises, J. Geophys. Res. 76 (2) (1971) 537–544.
[5] R.K. Dunne, E. O'Riordan, G.I. Shishkin, Singularly perturbed parabolic problems on non-rectangular domains, in: International Conference on Numerical Analysis and its Applications, Springer, 2000, pp. 265–272.
[6] R. Vulanović, P.A. Farrell, Continuous and numerical analysis of a multiple boundary turning point problem, SIAM J. Numer. Anal. 30 (5) (1993) 1400–1418.
[7] J.J.H. Miller, E. O'Riordan, G.I. Shishkin, Fitted Numerical Methods for Singular Perturbation Problems: Error Estimates in the Maximum Norm for Linear Problems in One and Two Dimensions, World Scientific, 2012.
[8] P. Farrell, A. Hegarty, J.J.H. Miller, E. O'Riordan, G.I. Shishkin, Robust Computational Techniques for Boundary Layers, CRC Press, 2000.
[9] G.I. Shishkin, L.P. Shishkina, Difference Methods for Singular Perturbation Problems, Chapman and Hall/CRC, 2008.
[10] R.K. Dunne, E. O'Riordan, G.I. Shishkin, A fitted mesh method for a class of singularly perturbed parabolic problems with a boundary turning point, Comput. Methods Appl. Math. 3 (3) (2003) 361–372.
[11] C. Clavero, J.L. Gracia, G.I. Shishkin, L.P. Shishkina, Grid approximation of a singularly perturbed parabolic equation with degenerating convective term and discontinuous right-hand side, Int. J. Numer. Anal. Model. 10 (4).
[12] S. Yadav, P. Rai, K.K. Sharma, A higher order uniformly convergent method for singularly perturbed parabolic turning point problems, Numer. Methods Partial Differential Equations 36 (2) (2020) 342–368.
[13] W. Huang, R.D. Russell, Adaptive Moving Mesh Methods, Vol. 174, Springer Science & Business Media, 2010.
[14] J. Mackenzie, Uniform convergence analysis of an upwind finite-difference approximation of a convection–diffusion boundary value problem on an adaptive grid, IMA J. Numer. Anal. 19 (2) (1999) 233–249.
[15] W. Huang, R.D. Russell, Analysis of moving mesh partial differential equations with spatial smoothing, SIAM J. Numer. Anal. 34 (3) (1997) 1106–1126.

[16] Y. Qiu, D. Sloan, Analysis of difference approximations to a singularly perturbed two-point boundary value problem on an adaptively generated grid, J. Comput. Appl. Math. 101 (1–2) (1999) 1–25.
[17] G. Beckett, J. Mackenzie, Convergence analysis of finite difference approximations on equidistributed grids to a singularly perturbed boundary value problem, Appl. Numer. Math. 35 (2) (2000) 87–109.
[18] N. Kopteva, N. Madden, M. Stynes, Grid equidistribution for reaction–diffusion problems in one dimension, Numer. Algorithms 40 (3) (2005) 305–322.
[19] G. Beckett, J. Mackenzie, On a uniformly accurate finite difference approximation of a singularly perturbed reaction–diffusion problem using grid equidistribution, J. Comput. Appl. Math. 131 (1–2) (2001) 381–405.
[20] P. Das, J. Vigo-Aguiar, Parameter uniform optimal order numerical approximation of a class of singularly perturbed system of reaction diffusion problems involving a small perturbation parameter, J. Comput. Appl. Math. 354 (2019) 533–544.
[21] P. Das, V. Mehrmann, Numerical solution of singularly perturbed convection–diffusion-reaction problems with two small parameters, BIT Numer. Math. 56 (1) (2016) 51–76.
[22] S. Gowrisankar, S. Natesan, The parameter uniform numerical method for singularly perturbed parabolic reaction–diffusion problems on equidistributed grids, Appl. Math. Lett. 26 (11) (2013) 1053–1060.
[23] C. Clavero, J.C. Jorge, F. Lisbona, A uniformly convergent scheme on a nonuniform mesh for convection–diffusion parabolic problems, J. Comput. Appl. Math. 154 (2) (2003) 415–429.
[24] B. Bujanda, C. Clavero, J.L. Gracia, J.C. Jorge, A high order uniformly convergent alternating direction scheme for time dependent reaction–diffusion singularly perturbed problems, Numer. Math. 107 (1) (2007) 1–25.
[25] C. Clavero, J.C. Jorge, F. Lisbona, G.I. Shishkin, A fractional step method on a special mesh for the resolution of multidimensional evolutionary convection–diffusion problems, Appl. Numer. Math. 27 (3) (1998) 211–231.
[26] C. de Boor, Good approximation by splines with variable knots, in: Spline Functions and Approximation Theory, Proceedings of the Symposium Held at the University of Alberta, Edmonton, Birkhauser, Basel, 1973.
[27] N. Kopteva, M. Stynes, A robust adaptive method for a quasi-linear one-dimensional convection–diffusion problem, SIAM J. Numer. Anal. 39 (4) (2001) 1446–1467.
[28] P. Das, Comparison of a priori and a posteriori meshes for singularly perturbed nonlinear parameterized problems, J. Comput. Appl. Math. 290 (2015) 16–25.
[29] N.M. Chadha, N. Kopteva, A robust grid equidistribution method for a one-dimensional singularly perturbed semilinear reaction–diffusion problem, IMA J. Numer. Anal. 31 (1) (2009) 188–211.
[30] X. Xu, W. Huang, R. Russell, J. Williams, Convergence of de boor's algorithm for the generation of equidistributing meshes, IMA J. Numer. Anal. 31 (2) (2011) 580–596.